5652–5659 *Nucleic Acids Research, 2008, Vol. 36, No. 17* *Published online 2 September 2008*
doi:10.1093/nar/gkn525

Thermodynamic analysis of 5′ and 3′ single- and 3′ double-nucleotide overhangs neighboring wobble terminal base pairs

Stacy Miller, Laura E. Jones, Karen Giovannitti, Dan Piper and Martin J. Serra*

Department of Chemistry, Allegheny College, 520 N. Main St, Meadville, PA 16335, USA

Received June 12, 2008; Revised July 30, 2008; Accepted July 31, 2008

ABSTRACT

Thermodynamic parameters are reported for duplex formation of 40 self-complementary RNA duplexes containing wobble terminal base pairs with all possible 3′ single and double-nucleotide overhangs, mimicking the structures of short interfering RNAs (siRNA) and microRNAs (miRNA). Based on nearest neighbor analysis, the addition of a single 3′ dangling nucleotide increases the stability of duplex formation up to 1 kcal/mol in a sequence-dependent manner. The addition of a second dangling nucleotide increases the stability of duplexes closed with wobble base pairs in an idiosyncratic manner. The results allow for the development of a nearest neighbor model, which improves the predication of free energy and melting temperature for duplexes closed by wobble base pairs with 3′ single or double-nucleotide overhangs. Phylogenetic analysis of naturally occurring miRNAs was performed. Selection of the effector miR strand of the mature miRNA duplex appears to be dependent on the orientation of the GU closing base pair rather than the identity of the 3′ double-nucleotide overhang. Thermodynamic parameters for the 5′ single terminal overhangs adjacent to wobble closing base pairs are also presented.

INTRODUCTION

Unpaired nucleotides, such as 3′ dangling ends, are important RNA secondary structural motifs. Understanding the thermostablity of RNA duplexes with 3′ dangling overhangs is essential for the understanding of the roles of this structure. For example, in the functioning of small RNAs, such as siRNA (short interfering RNAs) and miRNA (micro RNAs), the stability of the duplex ends are important determinants in the selection of the biologically relevant strand. Sequence-specific gene silencing is induced by siRNA (1–3). Most commonly used siRNA duplexes (guide/passenger) consist of two 21 nucleotide complementary strands terminated with a 3′ double-nucleotide overhang (4–9). miRNA is processed from a large RNA hairpin termed pri-miRNA. The final product is also a 21-nt complementary duplex (miR/miR*) with a 3′ double-nucleotide overhang. Both the siRNA (guide) and miRNA (miR) strands are incorporated into the RNA induced silencing complex (RISC) in an asymmetric manner that is dependent upon the stability of the base pairing at the 5′-ends of each strand in the duplex (10,11). The unpaired nucleotides, such as 3′ dangling ends, are also important in determining the structure and stability of large non-coding RNAs. For example, the average length of a helical region in rRNAs is ~7 nt (12). Therefore, for large RNAs, the unpaired nucleotides adjacent to the helix terminal base pair play a large role in determining the folding and stability of the RNA.

Single and double-nucleotide overhangs at the 3′-ends of RNA duplexes with terminal Watson–Crick base pairs contribute to the stability of the duplex in a sequence-dependent manner (13–20). Conversely, 5′ overhangs on RNA duplexes with terminal Watson–Crick base pairs do not contribute significantly to the stability of the duplex (14,21–24). The differing effects of the 3′ and 5′ overhangs have been attributed to the different stacking interactions of the dangling base with the closing base pair due to the A-form helical geometry of RNA (23).

Wobble (GU) base pairs are the most prevalent non-Watson–Crick motif in RNA (25,26). The geometry of the wobble base pair is markedly different than the geometry of canonical Watson–Crick base pairs (27,28). The unique geometric arrangement of the wobble base pair influences the stability of the secondary structural motifs adjacent to the wobble. For example, the stability of symmetric internal loops with a closing GU base pair are more sequence dependent than similar loops closed by Watson–Crick base pairs (29). RNA hairpin loops also display different stability when the loop is closed with a Watson–Crick or a wobble base pair. In particular, the most striking difference is that while the stacking interaction of the

*To whom correspondence should be addressed. Tel: +1 814 332 5356; Fax: +1 814 332 2789; Email: mserra@allegheny.edu

first mismatch of the loop on the closing base pair affects the stability of the hairpin loops closed by Watson–Crick base pair, for hairpin loops closed by wobble base pairs the stacking of the first mismatch on the wobble base pair does not affect the stability of the hairpin loop (30–32). The stability of bulge loops is also influenced differentially depending upon whether the bulge loop is closed with Watson–Crick or wobble base pairs. In this instance, both the 3′ or 5′ position of the bulge and orientation (G/U or U/G) of the wobble base pair affects the stability of the bulge (33). On the other hand, asymmetric internal loops closed by wobble base pairs are approximated well by assuming a AU base closure (29). In these examples, the wobble pair is constrained by being located in the interior of a helix or by the hairpin loop. The energy of stacking of terminal mismatches on a wobble base pair at the end of a helix is similar to the energy of stacking of terminal mismatches on Watson–Crick base pairs (32). Therefore, it seems that the less stained (constrained) a wobble base pair is the more closely its interactions mimic those of Watson–Crick base pairs.

While wobble base pairs are known to occur frequently at the termini of duplexes in RNA (25–27), little is known about the influence of dangling ends on these helices. Only one measurement of a 3′ dangling end on a duplex with a terminal wobble base pair has been reported. For the sequence $\binom{5'UA}{3'G}$, the 3′ dangling A was found to contribute ~1 kcal/mol to the stability of the duplex (34), similar to the contribution of a 3′ dangling A on Watson–Crick base pairs. The lack of data on the influence of 3′ single and double-nucleotide overhangs on duplexes closed by wobble base pair hinders the ability to predict the stability of the 5′-ends of siRNA and miRNA; limiting the ability to predict strand selection by the RISC complex and the stability of RNA in general.

We have shown previously that for duplexes closed by Watson–Crick base pairs, the addition of the second 3′ nucleotide of the type $\binom{5'RRY}{3'Y}$ and $\binom{5'YRX}{3'R}$, where R is a purine, Y is a pyrimidine and X is any base, contributes 0.5 kcal/mol to the stability of the RNA duplex (20). We used the results to develop a refined nearest neighbor model to predict the stability of RNA duplexes with 3′ double-nucleotide overhangs.

This article presents the thermodynamic parameters of the complete set of 3′ single and double-nucleotide dangling ends on duplexes closed by wobble base pairs. We find that the effects of the second 3′ dangling end is small and sequence dependent. The thermodynamic parameters obtained from this study are shown to improve the prediction of stability of an RNA duplex closed by wobble base pairs with 3′ double-nucleotide dangling end.

MATERIALS AND METHODS

RNA Synthesis and Purification

All oligomers were synthesized on CPG solid supports (Applied Biosystems 392 DNA/RNA Synthesizer, Foster City, CA) with phosphoramidites with the 2′ hydroxyl protected as the *tert*-butyl dimethylsilyl ether from Proligo. Oligomers underwent ammonia and fluoride deprotection; and, crude sample was purified using preparative thin layer chromatography (TLC) (*n*-propanol : ammonium hydroxide : water, 55 : 35 : 10) and Sep-Pak C18 (Waters, Milford, MA) chromatography as previously described (35). Sample purity was determined by HPLC (C-18) and was >95%.

Melting Curve and Data Analysis

Optical melting experiments were performed using a Beckman DU 800 Spectrophotometer and High Performance Temperature Controller at 260 or 280 nm. Absorbance changes for oligomers in 1 M NaCl melt buffer (1 M NaCl, 0.01 M sodium cacodylate, 0.001 M ethylenediamine tetraacetic acid, pH 7.0) were recorded as function of temperature from 90°C to 5°C at a rate of 1°C/min as described previously (35). Absorbance changes recorded from low to high temperature gave identical results indicative of the reversible nature of the helix to coil transition. The experiment was repeated at 10 varying sample concentrations to give at least a 50-fold concentration range (10 μM to 1 mM) for each sample. Absorbance versus temperature profiles were fit to a two-state model with sloping base lines using a nonlinear least squares program (36). Thermodynamic parameters for the oligomers were determined from both the average of the individual melt curves and plots of the reciprocal melting temperature (T_m^{-1}) versus $\ln(C_t)$ for self-complementary sequences or (T_m^{-1}) versus $\ln(C_t/4)$ for nonself-complementary sequences.

Phylogenetic analysis

A total of 1290 experimentally validated miRNA sequences from miRBase release 8.0 (http://microrna.sanger.ac.uk/sequences/; February 2006) (37,38) were 'conceptually diced' using an algorithm, which 'dices' the pri-miRNA sequences based on a 19-nt region of base pairing with a 3′ double-nucleotide overhang. These mature miRNA sequences were then analyzed for the frequency of wobble closing base pairs with 3′ double-nucleotide overhangs. Of the 1290 sequences, 257 fit our criteria. The occurrence of each of the possible combinations of wobble closing base pairs with double-nucleotide overhang on both the miR and miR* strands of the mature miRNA sequences was determined.

RESULTS AND DISCUSSION

Thermodynamic data

The measured thermodynamic parameters for the eight 3′ single-nucleotide terminal overhangs and 32 3′ double-nucleotide overhangs adjacent to wobble (GU) closing base pairs are presented in Table 1. Thermodynamic parameters were determined using both melt curve analysis and the T_m dependence models (36). Data from both models agreed within 15% for all sequences, consistent with the two-state model (17,39,40), with the exception of $(UGGCCGAG)_2$, $(UGGCCGAU)_2$ and $(GGCGCUUU)_2$. The average deviations in thermodynamic parameter values are 7.9%, 8.8% and 2.9% for ΔH^o, ΔS^o and ΔG^o_{37}, respectively.

Table 1. Thermodynamic parameters for duplex formation in 1 M NaCl[a]

Sequences	Average of curve fits				T_m^{-1} versus log C_t plots			
	$-\Delta H^o$ (kcal/mol)	$-\Delta S^o$ (e.u.)	$-\Delta G^o_{37}$ (kcal/mol)	T_m[b] (°C)	$-\Delta H^o$ (kcal/mol)	$-\Delta S^o$ (e.u.)	$-\Delta G^o_{37}$ (kcal/mol)	T_m[b] (°C)
(UGGCCG**AA**)$_2$	53.2 ± 1.1	140.5 ± 3.2	9.6 ± 0.1	61.9	55.1 ± 3.3	146.2 ± 9.9	9.7 ± 0.2	61.7
(UGGCCG**AG**)$_2$	*52.9 ± 2.1*	*139.8 ± 6.0*	*9.6 ± 0.2*	*61.7*	*64.8 ± 3.1*	*175.8 ± 9.3*	*10.2 ± 0.2*	*60.5*
(UGGCCG**AC**)$_2$	52.1 ± 0.8	137.8 ± 2.2	9.3 ± 0.2	60.4	60.5 ± 3.4	163.1 ± 10.2	9.9 ± 0.2	60.1
(UGGCCG**AU**)$_2$	*54.1 ± 1.0*	*143.1 ± 2.8*	*9.7 ± 0.2*	*62.1*	*64.0 ± 2.5*	*173.1 ± 7.6*	*10.3 ± 0.2*	*61.2*
(UGGCCG**A**)$_2$	52.4 ± 1.1	139.5 ± 3.4	9.2 ± 0.1	59.1	60.8 ± 1.1	164.9 ± 3.3	9.7 ± 0.1	58.9
(UGGCCG**GA**)$_2$	57.4 ± 3.5	153.2 ± 10.7	9.9 ± 0.3	61.4	62.0 ± 4.0	167.4 ± 12.1	10.1 ± 0.2	61.0
(UGGCCG**GG**)$_2$	51.9 ± 1.4	137.3 ± 4.4	9.3 ± 0.1	60.5	53.2 ± 1.4	141.4 ± 4.1	9.4 ± 0.1	60.2
(UGGCCG**GC**)$_2$	55.5 ± 5.7	143.6 ± 5.7	11.0 ± 0.2	69.8	56.0 ± 3.3	145.2 ± 9.7	11.0 ± 0.3	69.5
(UGGCCG**GU**)$_2$	47.9 ± 4.1	124.7 ± 12.3	9.2 ± 0.3	62.0	52.0 ± 5.7	137.3 ± 17.4	9.5 ± 0.4	61.4
(UGGCCG**G**)$_2$	52.2 ± 3.1	139.2 ± 9.7	9.0 ± 0.2	58.3	57.5 ± 4.6	155.4 ± 14.0	9.3 ± 0.3	58.0
(UGGCCG**CA**)$_2$	54.2 ± 1.2	142.9 ± 3.8	9.9 ± 0.1	63.2	62.5 ± 0.7	167.8 ± 2.0	10.5 ± 0.0	62.9
(UGGCCG**CG**)$_2$	56.1 ± 2.0	149.2 ± 6.3	9.8 ± 0.0	61.9	65.6 ± 1.6	177.8 ± 4.8	10.5 ± 0.1	61.3
(UGGCCG**CC**)$_2$	54.4 ± 1.1	143.2 ± 3.5	10.0 ± 0.1	63.9	61.4 ± 2.0	164.4 ± 6.2	10.5 ± 0.1	63.2
(UGGCCG**CU**)$_2$	54.9 ± 1.7	145.6 ± 5.3	9.8 ± 0.1	61.8	55.9 ± 2.6	148.6 ± 7.8	9.8 ± 0.1	61.6
(UGGCCG**C**)$_2$	55.4 ± 0.9	147.1 ± 2.9	9.8 ± 0.1	62.0	63.2 ± 1.9	170.5 ± 5.6	10.3 ± 0.1	61.5
(UGGCCG**UA**)$_2$	52.3 ± 2.3	138.0 ± 7.2	9.5 ± 0.2	61.6	57.8 ± 1.9	154.7 ± 5.8	9.8 ± 0.1	61.1
(UGGCCG**UG**)$_2$	53.0 ± 3.8	140.4 ± 11.7	9.4 ± 0.2	60.6	54.5 ± 1.9	145.2 ± 5.9	9.4 ± 0.1	60.0
(UGGCCG**UC**)$_2$	53.1 ± 1.5	140.5 ± 4.8	9.6 ± 0.1	61.4	57.9 ± 1.5	155.1 ± 4.5	9.8 ± 0.1	60.9
(UGGCCG**UU**)$_2$	52.8 ± 2.1	139.5 ± 6.2	9.5 ± 0.2	61.3	57.0 ± 2.6	152.2 ± 8.0	9.7 ± 0.2	60.9
(UGGCCG**U**)$_2$	51.6 ± 2.5	136.9 ± 7.4	9.1 ± 0.3	59.1	59.8 ± 3.5	162.0 ± 10.8	9.6 ± 0.2	58.8
(GGCGCU**AA**)$_2$	67.6 ± 2.9	181.0 ± 8.8	11.4±.27	65.7	69.7 ± 5.5	187.4 ± 16.5	11.5 ± 0.4	65.4
(GGCGCU**AG**)$_2$	63.8 ± 8.7	172.0 ± 26.8	10.5 ± 0.4	62.1	67.8 ± 10.6	183.8 ± 31.6	10.8 ± 0.8	62.2
(GGCGCU**AC**)$_2$	68.2 ± 2.6	183.4 ± 7.9	11.3 ± 0.4	64.7	65.3 ± 6.6	174.7 ± 20.1	11.1 ± 0.5	65.1
(GGCGCU**AU**)$_2$	60.6 ± 6.1	161.1 ± 18.4	10.6 ± 0.4	64.7	61.7 ± 3.6	164.5 ± 10.9	10.7 ± 0.2	64.3
(GGCGCU**A**)$_2$	60.9 ± 2.8	163.8 ± 8.6	10.2 ± 0.2	61.7	62.9 ± 3.8	169.8 ± 11.4	10.3 ± 0.2	61.4
(GGCGCU**GA**)$_2$	65.4 ± 2.1	177.1 ± 6.4	10.5 ± 0.2	61.5	74.4 ± 3.5	204.3 ± 10.7	11.1 ± 0.2	61.3
(GGCGCU**GG**)$_2$	61.9 ± 6.1	165.3 ± 18.2	10.6 ± 0.5	64.0	60.9 ± 5.3	162.6 ± 16.0	10.5 ± 0.4	63.7
(GGCGCU**GC**)$_2$	66.7 ± 2.9	179.7 ± 8.9	11.0 ± 0.2	63.7	75.8 ± 2.9	206.9 ± 8.8	11.6 ± 0.2	63.3
(GGCGCU**GU**)$_2$	60.3 ± 7.1	159.7 ± 21.5	10.8 ± 0.6	65.7	60.2 ± 4.9	159.4 ± 14.7	10.8 ± 0.3	65.7
(GGCGCU**G**)$_2$	65.4 ± 1.7	177.9 ± 5.6	10.3 ± 0.2	60.3	72.6 ± 10.3	199.8 ± 31.4	10.6 ± 0.5	59.8
(GGCGCU**CA**)$_2$	61.3 ± 6.5	165.9 ± 20.0	9.8 ± 0.3	59.4	65.6 ± 4.4	179.2 ± 13.6	10.1 ± 0.2	59.1
(GGCGCU**CG**)$_2$	57.8 ± 6.8	154.9 ± 20.0	9.7 ± 0.6	60.2	61.9 ± 4.8	167.4 ± 14.6	10.0 ± 0.3	60.4
(GGCGCU**CC**)$_2$	62.9 ± 6.4	170.2 ± 19.8	10.1 ± 0.4	60.4	59.6 ± 4.2	159.9 ± 12.8	9.9 ± 0.2	61.1
(GGCGCU**CU**)$_2$	57.8 ± 2.3	155.6 ± 6.7	9.5 ± 0.3	59.0	61.7 ± 5.4	167.6 ± 16.3	9.8 ± 0.3	58.9
(GGCGCU**C**)$_2$	63.4 ± 5.6	172.3 ± 16.7	9.9 ± 0.5	59.3	60.0 ± 6.0	162.2 ± 18.4	9.7 ± 0.3	59.4
(GGCGCU**UA**)$_2$	56.4 ± 9.6	150.0 ± 29.7	9.9 ± 0.5	62.0	55.7 ± 2.6	148.2 ± 7.9	9.7 ± 0.2	61.3
(GGCGCU**UG**)$_2$	59.0 ± 2.4	159.7 ± 7.6	9.5 ± 0.1	58.4	60.0 ± 4.1	164.7 ± 12.5	9.6 ± 0.2	58.2
(GGCGCU**UC**)$_2$	57.7 ± 3.8	155.4 ± 11.7	9.5 ± 0.2	58.0	63.4 ± 3.6	172.7 ± 10.9	9.8 ± 0.2	58.5
(GGCGCU**UU**)$_2$	*54.8 ± 5.7*	*147.6 ± 17.7*	*9.0 ± 0.3*	*56.9*	*65.5 ± 5.2*	*180.5 ± 16.1*	*9.5 ± 0.3*	*56.2*
(GGCGCU**U**)$_2$	57.3 ± 4.1	154.4 ± 12.5	9.4 ± 0.3	58.7	61.0 ± 5.1	165.7 ± 15.3	9.6 ± 0.3	58.6

[a]Solutions are 1.0 M NaCl, 10 mM sodium cacodylate, 0.5 mM EDTA pH 7.
[b]Calculated at 10^{-4} M oligomer concentration.
Thermodynamic values for $(UGGCCG)_2$ are −51.4 kcal/mol, −138.5 e.u. and −8.4 kcal/mol for, ΔH^o, ΔS^o, and ΔG^o_{37}, respectively and for $(GGCGCU)_2$ are −56.2 kcal/mol, −153.8, e. u. and −8.5 kcal/mol for ΔH^o, ΔS^o and ΔG^o_{37}, respectively (34).
Values in bold are 3′ overhangs, values in italics are non-two-state.

Free-energy parameters for 3′-terminal dangling ends adjacent to wobble base pairs

The thermodynamics for duplex formation for the core sequences $(UGGCCG)_2$ and $(GGCGCU)_2$ have been determined previously (34). The addition of a 3′ dangling end adjacent to a terminal wobble base pair increases the stability of the duplex by an average of 4.7°C and 6.9°C for a 10^{-4} M solution of (UGGCCG) and $(GGCGCU)_2$, respectively (Table 1). The free-energy increment for the addition of a 3′-terminal dangling end is currently approximated by the values of the corresponding 3′ dangling end adjacent to the measured values on duplexes closed by Watson–Crick base pairs (41). In order to determine the stability contributed by the 3′ dangling nucleotide on duplexes closed by wobble base pairs, the differences in the thermodynamic values between the sequences studied and the corresponding core sequences were determined using equations similar to Equation (1).

$$\Delta\Delta G^o_{37}3'X = 1/2(\Delta G^o_{37}\ (UGGCCGX)_2 - \Delta G^o 7_{37}\ (UGGCCG)_2) \quad \mathbf{1}$$

These results are summarized in Table 2. We have assumed no interaction between the overhangs at the

Table 2. Stabilization by addition of 3′ dangling nucleotide in 1 M NaCl to duplexes closed with wobble base pairs

	$-\Delta\Delta H^{oa}$ (kcal/mol)	$-\Delta\Delta S^{oa}$ (e.u.)	$-\Delta\Delta G_{37}{}^{oa}$ (kcal/mol)		$-\Delta\Delta H^{oa}$ (kcal/mol)	$-\Delta\Delta S^{oa}$ (e.u.)	$-\Delta\Delta G_{37}{}^{oa}$ (kcal/mol)
UA	2.9	6.5	0.9	**GA**	2.6	6.8	0.5
G	6.6	17.8	1.1	**U**	4.9	13.2	0.8
UC	2.8	6.7	0.7	**GC**	4.0	10.2	0.8
G	2.4	6.2	0.4	**U**	0.9	1.2	0.5
UG	6.4	17.5	1.0	**GG**	1.7	4.4	0.4
G	7.2	19.3	1.2	**U**	5.5	15.0	0.8
UU	1.5	3.1	0.5	**GU**	2.2	5.4	0.5
G	4.8	13.6	0.6	**U**	2.3	5.4	0.6

[a]Values calculated as described in text. Top row, this study; bottom row predicted as described by (41).

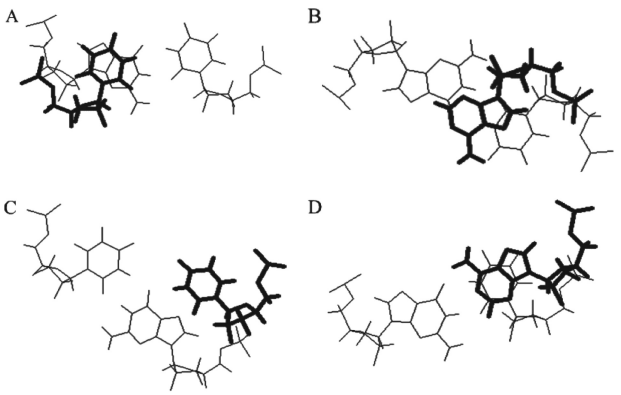

Figure 1. Stacking of bases on wobble GU base pairs. (**A**) View down the helix axis of $\binom{5'GU}{3'U}$ (**B**) View down helix axis of $\binom{5'UA}{3'G}$. (**C**) View down helix axis of $\binom{5'AU}{3'G}$. (**D**) View down helix axis of $\binom{5'AU}{3'G}$. The dangling bases are shown as the nearer base and are drawn in bold. Examples are taken from the NMR structure of the P1 helix of the group I intron (44).

two ends of the helix, hence we have taken half of the free-energy increment for the two dangling ends as the contribution of a single dangling end. Nonneighbor interactions have not been observed with short helices with single nucleotide overhangs (13–15,18–20) and the thermodynamic stability of nonself-complementary oligomers had been shown to be predicted with the thermodynamic values derived from self-complementary oligomers (18–20). The stability provided by the 3′ dangling ends on wobble terminal base pairs is similar to the stability of the corresponding 3′ dangling end on a helix terminated by Watson–Crick base pairs. Similar results were observed for the stabilization of helices with 3′ dangling 2-aminopurine. The stabilization for helices by the addition of a 3′ dangling 2-aminopurine was nearly the same for duplexes with terminal Watson–Crick or wobble base pairs (42). There is very good agreement between the values measured here and the previously predicted values. For example, the average difference in free energy between measured and previously predicted is 0.1 kcal/mol; and, the largest difference is only 0.4 kcal/mol. There are no known structures for a 3′ dangling end on a duplex closed by a wobble base pair [the structure of a wobble pair that closes an RNA hairpin is known (43) but in this case, it appears that the wobble base pair is strained by the small 3-nt hairpin loop]; so, we chose to examine the stacking of a 3′ nucleotide (as part of an adjacent base pair) on an isolated interior wobble base pair (44). Figure 1A and B display the stacking of a 3′ nucleotide on a wobble base pair. In both the cases, $\binom{5'GU}{3'U}$ and $\binom{5'UA}{3'G}$, the 3′ nucleotide is located directly above the wobble base pair. While this stacking was observed in the interior of a helix, where the 3′ nucleotide was part of a Watson–Crick base pair, the likelihood is that a 3′ dangling base at the end of a helix would have additional conformational plasticity and would be able to stack as well on a terminal wobble base pair. A 3′ dangling 2-aminopurine was shown to be primarily in the stacked orientation with both Watson–Crick and wobble terminal base pairs (42). The helix stabilization by 3′ dangling ends has been related to the strengthening of the hydrogen bonds in the terminal base pair provided by the shielding of the terminal base pair from the solvent by the dangling end (45).

Nearest neighbor analysis and free-energy parameters for 3′ dangling double-nucleotide overhangs adjacent to wobble base pairs

The addition of a second 3′ dangling nucleotide has only a minimal impact on the thermal stability of the RNA duplexes with terminal wobble base pairs. The average melting temperature increases by an average 2°C for a 10^{-4} M solution relative to the duplex with a single 3′-terminal overhang (Table 1). This increase in melting temperature is slightly less than that observed for the addition of a second 3′ dangling nucleotide addition to a helix closed by a Watson–Crick base pair (20).

In order to determine the stability contributed to the duplex by the second 3′ dangling nucleotide, differences in the thermodynamic values between the sequences studied and the corresponding sequence containing only the first overhanging nucleotide were also determined for all of the oligomers tested using equations similar to Equation (2).

$$\Delta\Delta G^{o}_{37}3'XY = \frac{1}{2}(\Delta G^{o}_{37}(UGCGXY)_2 - \Delta G^{o}_{37}(UGGCCGX)_2) \quad \mathbf{2}$$

These results are presented in Table 3. In general, the influence of the second 3′ dangling nucleotide is larger when the first 3′ dangling is a purine. The influence of the second 3′ dangling nucleotide on duplexes with terminal wobble base pairs is smaller and more idiosyncratic than the influence observed at the end of duplexes closed with Watson–Crick base pairs (20). The average error in measurement of the free energy for duplex formation of the oligomers in Table 1 is ~0.3 kcal/mol. The influence of the second 3′ dangling end is small and in most cases not significantly greater than the error in our measurements. Only five of the free-energy increments for the addition of the second 3′ dangling nucleotide to the duplexes in Table 1 are greater than the error in measurements. These values are indicated in bold in Table 3. The remaining values in Table 3 are best approximated by zero.

Table 3. Stabilization by addition of second 3′ dangling nucleotide in 1 M NaCl

$\Delta\Delta G_{37}^{o}$ (kcal/mol) values for addition of second 3′ overhang[a]

UGGCCG**XZ**

X	Z A	G	C	U
A	−0.1	*−0.2*	−0.1	*−0.2*
G	**−0.4**	−0.1	**−0.9**	−0.1
C	−0.0	−0.0	−0.1	+0.2
U	−0.2	−0.0	−0.2	−0.1

GGCGCU**XZ**

A	**−0.6**	−0.2	**−0.4**	−0.2
G	−0.2	−0.1	**−0.4**	−0.2
C	−0.1	−0.0	−0.1	+0.1
U	−0.2	−0.0	−0.1	*+0.1*

$\Delta\Delta H^{o}$(kcal/mol) values for addition of second 3′ overhang[a]

UGGCCG**XZ**

X	Z A	G	C	U
A	+1.2	*−1.2*	+0.2	*−1.2*
G	**−2.4**	+1.2	**−0.4**	+2.4
C	+0.4	−0.8	+0.7	+2.0
U	+0.3	+1.0	+0.1	+0.4

GGCGCU**XZ**

A	**−3.4**	−2.0	**−2.4**	+0.4
G	−0.4	+3.8	**−1.2**	+4.4
C	−0.9	+0.9	+0.2	+1.0
U	+1.6	−0.2	−0.7	*−0.5*

$\Delta\Delta S^{o}$ (e.u.) values for addition of second 3′ overhang[a]

UGGCCG**XZ**

X	Z A	G	C	U
A	+4.4	*−2.8*	+0.8	*−3.0*
G	**−6.5**	+4.0	**+1.5**	+8.2
C	+1.7	−2.4	+2.5	+5.8
U	+1.6	+3.4	+0.8	+1.8

GGCGCUXZ

A	**−8.7**	−5.6	**−6.2**	+2.0
G	−0.9	+12.4	**−2.3**	+14.6
C	−2.6	+3.0	+1.1	+2.8
U	+5.5	−1.0	−2.0	*−2.0*

[a]Values calculated as described in text. Values not in bold are less than the errors in the measurement and considered to be zero. Values in italics are non-two-state.

To test the generality of conclusions from this work, thermodynamic parameters were also measured for five test sequences with 3′ double-nucleotide overhangs on different core sequences from those used to develop the model. The measured and predicted (both with and without the influence of the second 3′ dangling end) thermodynamic values for the five sequences are presented in Table 4. Note that the last two duplexes in Table 3 have 3′ double overhangs adjacent to Watson–Crick as well as wobble terminal base pairs. As observed previously for duplexes closed by Watson–Crick base pairs (20), inclusion of the contribution of the second 3′ dangling end improves the prediction of the stability, both in terms of ΔG^{o}_{37} and T_m. The prediction of the free energy for duplex formation improves by 0.5 kcal/mol relative to the measured values for the duplexes in Table 4. The average deviation from the measured free-energy values for duplex formation is about 0.35 kcal/mol with the inclusion of the free-energy increment for the second terminal mismatch. The prediction of the melting temperatures in Table 4 also improves with the inclusion of the contribution of the second 3′ dangling end, by 4.3°C.

Phylogenetic analysis of naturally occurring miR sequences

Phylogenetic analysis of experimentally determined miRNA sequences from the miRNA database revealed a total of 1290 strand sequences; 257 of these sequences were terminated with a wobble closing base pair and had 3′-terminal double-nucleotide overhang consisting of two of the four Watson–Crick bases. The miR strand of all the 257 miRNAs that we used in this study were experimentally cloned and sequenced; however, since the miR* of miRNA duplexes is degraded after the duplex is unwound and the miR strand is incorporated into RISC, the miR* sequences in the database have been predicted based upon the cloned and sequenced miR strand. Frequency of appearance of each of the 32 possible combinations (data not shown) of wobble closing base pairs neighboring 2-nt 3′ overhangs were determined for both miR and predicted miR* strands. The sequences were

Table 4. Measured and predicted thermodynamic parameters for test sequence duplex formation[a]

	Average of curve fits				T_m^{-1} *vs* log C_t plots			
Sequences	$-\Delta H^{o}$ (kcal/mol)	$-\Delta S^{o}$ (e.u.)	$-\Delta G^{o}$ (kcal/mol)	T_m[b] (°C)	$-\Delta H^{o}$ (kcal/mol)	$-\Delta S^{o}$ (e.u.)	$-\Delta G^{o}_{37}$ (kcal/mol)	T_m[b] (°C)
UGAGUAC	50.8	145.0	5.8	32.6	44.1	122.6	6.1	33.7
UUGCUCG	(35.2)	(98.0)	(4.8)	(22.6)				
	(37.6)	(104.2)	(5.2)	(27.2)				
UGAGUAA	54.5	156.9	5.8	33.0	41.6	115.3	5.9	32.3
GUGCUCG	(35.2)	(98.0)	(4.8)	(22.6)				
	(38.6)	(106.7)	(5.4)	(29.1)				
UGAGUUC	55.7	162.3	5.4	30.5	57.2	167.0	5.4	30.9
AGGCUCG	(34.9)	(98.2)	(4.5)	(19.6)				
	(37.3)	(104.7)	(4.9)	(23.6)				
UACAGGC	54.7	159.9	5.1	29.0	48.8	140.6	5.2	28.8
AAGUGUC	(41.0)	(117.2)	(4.7)	(23.5)				
	(43.5)	(123.9)	(5.2)	(27.0)				
UGCUGAU	49.9	142.6	5.6	31.6	53.8	155.1	5.7	32.1
UGACGAU	(39.8)	(112.5)	(4.9)	(25.6)				
	(42.3)	(119.2)	(5.4)	(28.6)				

[a]Solutions are 1.0 M NaCl, 10 mM sodium cacodylate, 0.5 mM EDTA pH 7.
[b]Calculated at 10^{-4} M oligomer concentration. Values in parenthesis are predicted: top row is the predicted values for single 3′ terminal overhang duplexes and bottom row is the predicted values as described in the text for duplexes with 3′ double overhangs.

divided into categories; results of this search are presented in Table 5. The small number of sequences in the database make it difficult to draw too fine a conclusion. The distribution of sequences into the miR or miR* strand was found to be related to the orientation of the wobble base pair at the end of the helix. When the helix is terminated with a G/U wobble base pair, the majority of sequences are found in the miR*; when the helix is terminated with a U/G wobble base pair, the majority of the sequences are found in miR. Since the influence of 3′ double-nucleotide overhangs on wobble base pairs have a relatively small influence on the stability of the helix, there is no clear sequence selection of the double overhangs sequences in the naturally occurring miR sequences.

Nearest neighbor analysis and free-energy parameters for 5′ dangling nucleotide overhangs adjacent to wobble base pairs

Addition of a 5′ dangling end to an RNA duplex has been shown to have only a very small increase in the stability of the RNA duplex (23,24). These results were rationalized by the fact that a 5′ nucleotide does not stack well on the adjacent Watson–Crick base pair. Since wobble base pairs have a different geometry, the stacking of a 5′ nucleotide may make a more significant contribution to the stability of helix when it is adjacent to a wobble base pair than to a Watson–Crick base pair. In fact, a 5′ base has been shown (in the context of an isolated interior wobble base pair) to stack well on an adjacent wobble base pair in an RNA helix (44). Figure 1 displays the stacking of a 5′ nucleotide on a wobble base pair. While the 5′ nucleotide of $\begin{pmatrix} 5'UG \\ 3'\ U \end{pmatrix}$ does not stack on the wobble base pair (Figure 1C), the 5′ nucleotide of $\begin{pmatrix} 5'AU \\ 3'\ G \end{pmatrix}$ displays excellent stacking on the wobble base pair (Figure 1D), where the adenosine is located directly above the neighboring uracil residue. To determine if the difference in stacking influences the ability of a 5′ dangling nucleotide to stabilize an RNA duplex, we investigated the influence of all possible wobble base pairs and 5′ dangling overhangs on the stability of a duplex. These results are presented in Table 6. Thermodynamic parameters were determined using both melt curve analysis and the T_m-dependent models (36). There is excellent agreement between the two methods of analysis. The average deviations in thermodynamic parameter values are 3.2%, 3.4% and 1.1% for ΔH^o, ΔS^o and $\Delta G^o{}_{37}$, respectively.

In order to determine the stability contributed by the 5′ dangling nucleotide on duplexes closed by wobble base pairs, the differences in the thermodynamic values between the sequences studied and the corresponding core sequences were determined using equations similar to Equation (3).

$$\Delta\Delta G^o_{37}5'\mathrm{X} = \frac{1}{2}(\Delta G^o_{37}(\mathbf{X}\mathrm{UGGCG})_2 - \Delta G^o_{37}(\mathrm{UGGCG})_2) \quad \mathbf{3}$$

These results are summarized in Table 7. The free-energy increment for the addition of a 5′ dangling end $\begin{pmatrix} 5'UG \\ 3'\ U \end{pmatrix}$ is larger than for $\begin{pmatrix} 5'UG \\ 3'\ U \end{pmatrix}$; surprisingly, the

Table 5. Phylogenetic analysis of 3′ double nucleotide overhangs in naturally occurring miRNAs[a]

Occurrence in miR or miR* strands in mature miRNAs	Total	
Sequence of 3′ double nt dangling ends	miR	miR*
5′—G-pur-X U—5′	13	69
5′—G-pyr-X U—5′	8	102
5′—U-pur-X 29 G—5′	29	9
5′—U-pyr-X G—5′	15	12

[a]Number of sequences in the database closed by a wobble base pair with the corresponding 3′ double overhang (total number = 257).

Table 6. Thermodynamic parameters for duplex formation in 1 M NaCl[a]

Sequences	Average of curve fits				$T_m{}^{-1}$ versus log C_t plots			
	$-\Delta H^o$ (kcal/mol)	$-\Delta S^o$ (e.u.)	$-\Delta G^o{}_{37}$ (kcal/mol)	$T_m{}^b$ (°C)	$-\Delta H^o$ (kcal/mol)	$-\Delta S^o$ (e.u.)	$-\Delta G^o{}_{37}$ (kcal/mol)	$T_m{}^b$ (°C)
(**A**UGGCCG)$_2$	46.8 ± 4.90	122.0 ± 15.	9.0 ± 0.3	60.3	44.8 ± 1.8	116.3 ± 5.6	8.8 ± 0.1	59.9
(**C**UGGCCG)$_2$	51.1 ± 1.8	135.2 ± 5.6	9.2 ± 0.1	59.7	50.2 ± 0.7	132.5 ± 2.0	9.1 ± 0.1	59.7
(**G**UGGCCG)$_2$	48.0 ± 2.8	126.0 ± 8.5	9.0 ± 0.2	59.7	49.2 ± 1.7	129.7 ± 5.3	9.0 ± 0.1	59.5
(**U**UGGCCG)$_2$	43.4 ± 6.2	111.9 ± 18.8	8.7 ± 0.5	60.2	42.3 ± 3.8	109.1 ± 11.6	8.5 ± 0.2	59.0
(UGGCCG)$_2$[c]	51.4	138.5	8.4					
(**A**GCCGGU)$_2$	55.9 ± 5.1	150.2 ± 15.7	9.3 ± 0.3	58.8	55.1 ± 4.4	147.8 ± 13.4	9.3 ± 0.3	58.7
(**C**GCCGGU)$_2$	57.9 ± 1.8	156.7 ± 21.5	9.3 ± 0.4	57.8	57.6 ± 4.8	156.0 ± 14.8	9.2 ± 0.3	57.5
(**G**GCCGGU)$_2$	57.2 ± 4.2	154.6 ± 3.3	9.2 ± 0.2	57.4	62.6 ± 2.5	171.4 ± 7.7	9.4 ± 0.1	56.9
(**U**GCCGGU)$_2$	53.8 ± 4.1	144.6 ± 12.5	9.0 ± 0.3	57.3	54.8 ± 3.4	147.7 ± 10.3	9.0 ± 0.2	57.0
(GCCGGU)$_2$[c]	58.8	159.6	9.2					

[a]Solutions are 1.0 M NaCl, 10 mM sodium cacodylate, 0.5 mM EDTA pH 7.
[b]Calculated at 10^{-4} M oligomer concentration.
[c]Ref. (34).

Table 7. Stabilization by addition of 5′ dangling nucleotide in 1 M NaCl to duplexes closed with wobble base pairs

	$-\Delta\Delta H^{oa}$ (kcal/mol)	$-\Delta\Delta S^{oa}$ (e.u.)	$-\Delta\Delta G_{37}{}^{oa}$ (kcal/mol)		$-\Delta\Delta H^{oa}$ (kcal/mol)	$-\Delta\Delta S^{oa}$ (e.u.)	$-\Delta\Delta G_{37}{}^{oa}$ (kcal/mol)
AU				**AG**			
G	−2.8	−9.7	0.2	**U**	−1.6	−5.3	0.1
CU				**CG**			
G	−0.4	−4.6	0.4	**U**	−0.5	−1.6	0.0
GU				**GG**			
G	−1.4	−5.3	0.3	**U**	0.6	1.7	0.1
AU				**UG**			
G	−4.3	−14.0	0.1	**U**	−2.2	−6.8	−0.1

[a]Values calculated as described in text.

effect is still small, on average 0.2 kcal/mol. While it is possible for the 5′ dangling nucleotide to stack on the terminal base pair, it has been shown that 5′ dangling nucleotide is a highly dynamic specie which is in the stacked conformation only a small amount of the time (42). Thus, a 5′ nucleotide does not provide significant stabilization to the duplex with a wobble closing base pair.

CONCLUSIONS

The influence of single 3′ dangling ends on the stability of duplex formation of helices with terminal wobble base pairs is nearly the same as for helices with terminal Watson–Crick base pairs. The addition of a second 3′ dangling end leads to stabilization of the duplex although to a lesser extent than the addition of the first 3′ dangling end. The addition of the second 3′ dangling end to a duplex with a terminal wobble base pair also increases the stability of the duplex less than with duplexes with Watson–Crick terminal base pairs. The influence of the second dangling end on the stability of the duplexes with terminal wobble base pairs is idiosyncratic, depending upon the orientation of the wobble base pair and the identity of the two dangling nucleotides. Inclusion of the contribution of the second dangling end improves the prediction of the stability of duplexes with 3′ double-nucleotide overhangs. Inclusion of the contribution of the 3′ double-nucleotide overhang contribution should improve the ability to predict strand selection by the RISC complex, and therefore improve our understanding and control of the miRNA and siRNA pathways.

ACKNOWLEDGEMENTS

We thank Herve Seitz for providing the 3′ double-nucleotide overhang miRNA data.

FUNDING

National Science Foundation (MCB-0340958); National Institutes of Health (RGM068426). Funding for open access charge: National Science Foundation.

Conflict of interest statement. None declared.

REFERENCES

1. Zamore,P.D., Tuschl,T., Sharp,P.A. and Bartel,D.P. (2000) RNAi: double-stranded RNA directs the ATP-dependent cleavage of mRNA at 21 to 23 nucleotide intervals. *Cell*, **101**, 25–33.
2. Elbashir,S.M., Harborth,J., Lendeckel,W., Yalcin,A., Weber,K. and Tuschl,T. (2001) Duplexes of 21-nucleotide RNAs mediate RNA interference in cultured mammalian cells. *Nature*, **411**, 494–498.
3. Fire,A., Xu,S., Montgomery,M.K., Kostas,S.A., Driver,S.E. and Mello,C.C. (1998) Potent and specific genetic interference by double-stranded RNA in Caenorhabditis elegans. *Nature*, **391**, 806–811.
4. Elbashir,S.M., Lendeckel,W. and Tuschl,T. (2001) RNA interference is mediated by 21- and 22-nucleotide RNAs. *Genes Dev.*, **15**, 188–200.
5. Hamilton,A.J. and Baulcombe,D.C. (1999) A species of small anti-sense RNA in posttranscriptional gene silencing in plants. *Science*, **286**, 950–952.
6. Hammond,S.M., Caudy,A.A. and Hannon,G.J. (2001) Post-transcriptional gene silencing by double-stranded RNA. *Nat. Rev. Genet.*, **2**, 110–119.
7. Bernstein,E., Caudy,A.A., Hammond,S.M. and Hannon,G. J. (2001) Role for a bidentate ribonuclease in the initiation step of RNA interference. *Nature*, **409**, 295–296.
8. Hutvágner,G., McLachlan,J., Pasquinelli,A.E., Balint,É., Tuschl,T. and Zamore,P.D. (2001) A cellular function for the RNA-interference enzyme Dicer in the maturation of the let-7 small temporal RNA. *Science*, **293**, 834–838.
9. Knight,S.W. and Bass,B.L. (2001) A role for the RNase III enzyme DCR-1 in RNA interference and germ line development in Caenorhabditis elegans. *Science*, **293**, 2269–2271.
10. Schwarz,D.S., Hutvágner,G., Du,T., Xu,Z., Aronin,N. and Zamore,P.D. (2003) Asymmetry in the assembly of the RNAi enzyme complex. *Cell*, **115**, 199–208.
11. Khvorova,A., Reynolds,A. and Jeyasena,S.D. (2003) Functional siRNAs and miRNAs exhibit strand bias. *Cell*, **115**, 209–216.
12. Turner,D.H., Sugimoto,N. and Freier,S.M. (1998) RNA structure prediction. *Annu. Rev. Biophys. Chem.*, **17**, 167–192.
13. Freier,S.M., Burger,B.J., Alkema,D., Neilson,T. and Turner,D.H. (1983) Effects of 3′ dangling end stacking on the stability of GGCC and CCGG double helices. *Biochemistry*, **22**, 6198–6206.
14. Petersheim,M. and Turner,D.H. (1983) Base-stacking and base-pairing contributions to helix stability: thermodynamics of double-helix formation with CCGG, CCGGp, CCGGAp, ACCGGp, CCGGUp, and ACCGGUp. *Biochemistry*, **18**, 256–263.
15. Sugimoto,N., Kierzek,R. and Turner,D.H. (1987) Sequence dependence for the energetics of dangling ends and terminal base pairs in ribonucleic acid. *Biochemistry*, **26**, 4554–4558.
16. Limmer,S., Hofmann,H.P., Ott,G. and Sprinzl,M. (1993) The 3′-terminal end (NCCA) of tRNA determines the structure and stability of the aminoacyl acceptor stem. *Proc. Natl Acad. Sci. USA*, **90**, 6199–6202.

17. Bibillo,A., Figlerowicz,M., Ziomek,K. and Kierzek,R. (2000) The nonenzymatic hydrolysis of oligoribonucleotides. VII. Structural elements affecting hydrolysis. *Nucleos. Nucleot. Nucl.*, **19**, 977–994.
18. Ohmichi,T., Nakano,S., Miyoshi,D. and Sugimoto,N. (2002) Long RNA dangling end has large energetic contribution to duplex stability. *J. Am. Chem. Soc. USA*, **124**, 10367–10372.
19. O'Toole,A.S., Miller,S. and Serra,M.J. (2005) Stability of 3′ double nucleotide overhangs which model the 3′ ends of siRNA. *RNA*, **11**, 512–516.
20. O'Toole,A.S., Miller,S., Haines,M., Zink,M.C. and Serra,M.J. (2006) Comprehensive thermodynamic analysis of 3′ double-nucleotide overhangs neighboring Watson-Crick terminal base pairs. *Nucleic Acids Res.*, **34**, 3338–3344.
21. Gennis,R.B. and Cantor,C.R. (1970) Optical properties of specific complexes between complementary oligoribonucleotides. *Biochemistry*, **9**, 4714–4725.
22. Alkema,D., Bell,R.A., Hader,P.A. and Neilson,T. (1981) Triplet GpCpA forms a stable RNA duplex. *J. Am. Chem. Soc. USA*, **103**, 2866–2868.
23. Freier,S.M., Alkema,D., Sinclair,A., Neilson,T. and Turner,D.H. (1985) Contributions of dangling end stacking and terminal base-pair formation to the stabilities of XGGCCp, XCCGGp, XGGCCYp, and XCCGGYp helixes. *Biochemistry*, **24**, 4533–4539.
24. Freier,S.M., Sugimoto,N., Sinclair,A., Alkema,D., Neilson,T., Kierzek,R., Caruthers,M.H. and Turner,D.H. (1986) Stability of XGCGCp, GCGCYp, and XGCGCYp Helixes—an empirical estimate of the energetics of hydrogen-bonds in nucleic-acids. *Biochemistry*, **25**, 3214–3219.
25. Gutell,R.R., Larson,N. and Woese,C.R. (1994) Lessons from an evolving rRNA: 16S and 23S rRNA structures form a comparative perspective. *Microbiol. Rev.*, **58**, 10–26.
26. Gautheret,D., Konings,D. and Gutell,R.R. (1995) G•U base paring motifs in ribosomal RNA. *RNA*, **1**, 807–814.
27. Mizuno,H. and Sundaralingam,M. (1978) Stacking of Crick wobble pair and Watson-Crick pair: stability rules of G-U pairs at ends of helical stems in tRNAs and the relation to codon-anticodon wobble interaction. *Nucleic Acids Res.*, **5**, 4451–4461.
28. Masquida,B. and Westhof,E. (2000) On the wobble GU and related pairs. *RNA*, **6**, 9–15.
29. Schroeder,S.J. and Turner,D.H. (2001) Thermodynamic stabilities of internal loops with GU closing pairs in RNA. *Biochemistry*, **40**, 11509–11517.
30. Serra,M.J., Lyttle,M.H., Axenson,T.J., Schadt,C.A. and Turner,D.H. (1993) RNA hairpin loop stability depends on closing base pair. *Nucleic Acids Res.*, **21**, 3845–3849.
31. Giese,M.R., Betschart,K., Dale,T., Riley,C.K., Rowan,C., Sprouse,K.J. and Serra,M.J. (1998) Stability of RNA hairpins closed by wobble base pairs. *Biochemistry*, **37**, 1094–1100.
32. Vecenie,C.J., Morrow,C.V., Zyra,A. and Serra,M.J. (2006) A study of the sequence dependence of stability of RNA hairpin molecules with six nucleotide loops. *Biochemistry*, **45**, 1400–1407.
33. Blose,J.M., Manni,M.L., Klapec,K.A., Stranger-Jones,Y., Zyra,A.C., Sim,V., Griffith,C.A, Long,J.D. and Serra,M.J. (2007) Non-nearest-neighbor dependence of the stability for RNA bulge loops based on the complete set of group I single-nucleotide bulge loops. *Biochemistry*, **46**, 15123–15135.
34. Freier,S.M., Kierzek,R., Caruthers,M.H., Neilson,T. and Turner,D.H. (1986) Free-energy contributions of G·U and other terminal mismatches to helix stability. *Biochemistry*, **25**, 3209–3213.
35. Serra,M.J., Axenson,T.J. and Turner,D.H. (1994) A model for the stabilities of RNA hairpins based on a study of the sequence dependence of stability for hairpins with six nucleotides. *Biochemistry*, **33**, 14289–14296.
36. McDowell,J.A. and Turner,D.H. (1996) Investigation of the structural basis for thermodynamic stabilities of tandem GU mismatches: solution structure of $(rGAG\underline{GU}CUC)_2$ by two-dimensional NMR and simulated annealing. *Biochemistry*, **35**, 14077–14089.
37. Griffiths-Jones,S. (2004) The microRNA registry. *Nucleic Acids Res.*, **32**, D109–D111.
38. Griffiths-Jones,S., Grocock,R.J., van Dongen,S., Bateman,A. and Enright,A.J. (2006) miRBase: microRNA sequences, targets and gene nomenclature. *Nucleic Acids Res.*, **34**, D140–D144.
39. Freier,S.M., Kierzek,R., Jaeger,J.A., Sugimoto,N., Caruthers,M.H., Neilson,T. and Turner,D.H. (1986) Improved free-energy parameters for predictions of RNA duplex stability. *Proc. Natl Acad. Sci. USA*, **83**, 9373–9377.
40. Allawi,H.T. and SantaLucia,J. Jr. (1997) Thermodynamics and NMR of internal G.T mismatches in DNA. *Biochemistry*, **36**, 10581–10594.
41. Jaeger,J.A., Turner,D.H. and Zuker,M. (1989) Improved predictions of secondary structures for RNA. *Proc. Natl Acad. Sci. USA*, **86**, 7706–7710.
42. Lui,J.D., Zhao,L. and Xia,T. (2008) The dynamic structural basis of differential enhancement of conformational stability by 5′ and 3′dangling ends in RNA. *Biochemistry*, **47**, 5962–5975.
43. Leper,T., Leulliot,N. and Varani,G. (2003) The solution structure of an essential stem-loop of human telomerase RNA. *Nucleic Acids Res.*, **31**, 2614–2621.
44. Allain,F.H. and Varani,G. (1995) Structure of the P1 helix from group I self-splicing introns. *J. Mol. Biol.*, **250**, 333–353.
45. Isaksson,J. and Chattopadhyaya,J. (2005) A uniform mechanism correlating dangling-end stabilization and stacking geometry. *Biochemistry*, **22**, 5390–5401.